The Korean Journal of Ceramics, **4** [3] 213 - 221 (1998)

Preparation of Proton-Conducting Gd-Doped Barium Cerate by Oxalate Coprecipitation Method

Yong-Sung Choi and Soo-Man Sim

School of Materials Science & Engineering, Hong-Ik University, Chochiwon 339-701, Korea
(Received May 13, 1998)

$BaCe_{0.9}Gd_{0.1}O_{2.95}$ powder was synthesized by oxalate coprecipitation method. Precipitate with a stoichiometric ratio of the cations was prepared by adding a mixture of Ba, Ce and Gd nitrate solutions to an oxalic acid solution at pH 4. Reaction between the constituent oxides to form a perovskite phase was initiated at 800°C and a single phase $BaCe_{0.9}Gd_{0.1}O_{2.95}$ powder having good sinterability was obtained after calcination at 1000°C. Sintering green compacts of this powder for 6 h showed a considerable densification to start at 1100°C and resulted in 93% and 97% relative densities at 1300° and at 1450°C, respectively. Whereas the powder compacts prepared by solid state reaction had lower relative densities, 78% at 1300°C and 90% at 1450°C. Fine particles of CeO_2 second phase were observed in the surfaces of the sintered compacts. This was attributed to the evaporation of BaO from the surface that had been exposed during thermal etching.

Key words : Barium cerate, High-temperature proton conductor, Oxalate coprecipitation, Powder synthesis, Sinterability

I. Introduction

Iwahara et al.[1] first reported that certain perovskite-type oxides based on $SrCeO_3$ exhibit proton conduction in an atmosphere containing hydrogen or water vapor at elevated temperatures. Since then, high-temperature proton conductors (HPTCs) have been extensively studied due to their potential applications in hydrogen gas sensors, fuel cells and steam electrolyzers.[2-4] Particularly, barium cerates doped with Nd, Gd or Y are interesting because of high proton conductivity and good structural and chemical stability at high temperatures.[5]

Proton conducting perovskite-type oxides are of form, $AB_{1-x}MO_{3-\alpha}$, where A is a divalent ion (Ba^{2+} or Sr^{2+}), B is a tetravalent ion (Ce^{4+} or Zr^{4+}), M is a trivalent rare earth dopant ion and α is the concentration of oxygen ion vacancies. Doping of barium cerate with Gd generates oxygen ion vacancies (V_o) in order to maintain electrical charge balance:

$$Gd_2O_3 \rightarrow 2Gd'_{Ce}+3O_o+V_o \quad (1)$$

Oxygen ion vacancies react with water vapor to form interstitial protons (H), which enter into the lattice and migrate by hopping from an oxygen ion to an adjacent one along OH-O bridge:

$$V_o+H_2O_{(g)} \rightleftarrows 2H+O_o \quad (2)$$

Oxygen ion vacancies also react with oxygen and produce holes (h). This reaction competes with the reaction above for the available oxygen ion vacancies:

$$V_o+1/2O_{2(g)} \rightleftarrows O_o+2h \quad (3)$$

Thus, HPTCs including Gd-doped barium cerate can exhibit proton and p-type conduction depending on water vapor pressure and oxygen partial pressure. It is generally accepted that proton conduction in doped barium cerates is gradually changed to oxygen ion conduction over a temperature range of 600°C to 1000°C, where the dissolution of proton is no longer possible.[6]

Despite many efforts to understand conduction mechanisms, less attention has been paid to the synthesis of HPTCs. Most researchers prepare HPTCs by solid state reaction that carbonate and oxides of the constituents are mixed, followed by calcination and sintering at high temperatures. Calcination is carried out at temperatures as high as 1400°C and repeated several times to obtain a single perovskite phase.[7-10] Such heat treatments result in an increase in particle size and forming agglomerates and make it difficult to achieve dense and homogeneous microstructures.

Oxalate coprecipitation method has been used to produce fine powders of doped barium cerates having good chemical homogeneity and sinterability.[11,12] Flint and Slade[11] prepared Ca and Gd-doped barium cerate powders from precipitates obtained by adding an excess ammonium oxalate to a mixture of nitrate solutions. Chen et al.[12] also prepared Nd-doped barium cerate powder in a similar way and studied its sinterability.

Recently, a few workers have investigated the influence of dopants and powder synthesis methods on reaction process, sintering behavior, and microstructures in an attempt to relate to the electrical properties of HPTCs.[12-16] However, sintering experiments and microstructural characterizations should be performed with care. For

example, the evaporation of BaO during high temperature sintering, which has been pointed out by Shima and Haile[15] and also observed in the present work, may alter a stoichiometry of the composition. In addition, the reported density values are not reliable because most densities were determined by simply measuring sample dimensions. The Archimedes method can not be used in measuring density since sintered barium cerate pellets have a tendency to disintegrate in a variety of liquids.[16]

In this study, Gd-doped barium cerate powder with a nominal composition of $BaCe_{0.9}Gd_{0.1}O_{2.95}$ was prepared by oxalate coprecipitation method. Its characteristics and sinterability were investigated and compared with those of powder prepared by solid state reaction.

II. Experimental Procedure

1. Coprecipitation of oxalates

Aqueous solutions containing 0.04M $Ba(NO_3)$ (99%, Aldrich, USA), 0.04M $Ce(NO_3) \cdot 6H_2O$ (99%, Aldrich, USA), 0.05M $Gd(NO_3) \cdot 6H_2O$ (99.9%, Aldrich, USA) and 0.075M oxalic acid (99.5%, Junsei Chemical, Japan) were prepared as stock solutions. In order to assure complete precipitation of all metal ions into oxalates, an optimum pH value of the solution of oxalic acid was determined by adding 15 ml of each nitrate solution to 30 ml of the oxalic acid solution at pH values varying from 1.3 to 7 and by measuring the amounts of the resulting precipitates.

The stock solutions were mixed in a 1:0.9:0.1 molar ratio of Ba : Ce : Gd. Precipitation was carried out by dropwise addition of a mixture of the nitrate solutions to the oxalic acid solution under vigorous stirring and stirring was continued for 4 h to complete precipitation reaction. The pH of the oxalic acid solution, prior to the addition of the nitrate solution, was adjusted to the predetermined pH value of 4 with NH_4OH and kept constant throughout the precipitation reaction.

The precipitates were separated using filter press (Millipore, USA) and filter paper (0.45 μm, Millipore, USA), washed several times with deionized water and then dried at 80°C for 4 h. The dried precipitates were stored in a vacuum desiccator to avoid contacts with H_2O and CO_2 in air.

2. Calcination and sintering

The precipitate was calcined at 1000°C for 10 h, dispersed in 99.9% pure ethanol by ultrasonication (Ultrasonic homogenizer, Cole-Parmer, USA) and milled with zirconia ball for 12 h. The powder was uniaxially cold pressed into pellets in 1 cm diameter at 93.5 MPa. Green compacts were sintered at temperatures between 1100° and 1450°C for 6 h in air at a heating rate of 10°C/min and cooled at a cooling rate of 5°C/min. In order to suppress the evaporation of BaO, the samples were embedded in $BaCeO_3$ powder throughout sintering.

In addition, powder was prepared by solid state reaction to compare with the powder prepared by oxalate coprecipitation. $BaCO_3$ (99%, Duksan, Korea), CeO_2 (99.9%, High Purity Chem., Japan), Gd_2O_3 (99.9%, Aldrich, USA) powders were mixed in a stoichiometric ratio of $BaCe_{0.9}Gd_{0.1}O_{2.95}$ and then ground in acetone with an agate mortar and pestle. The powder mixture was dried, calcined at 1250°C for 10 h and used in preparing green compacts.

3. Characterization

Thermal behavior of the precipitates was studied with thermogravimetry and differential thermal analysis (TG-DTA 2000, MAC Science, Japan) at a heating rate of 5°C/min up to 1400°C in air.

For phase identification, the precipitates were heated to temperatures between 400° and 1000°C in air at a heating rate of 5°C/min, held for 4 h and furnace-cooled to room temperature. Phases present in the powders were examined by X-ray powder diffraction (MAC Science M03XHF, Japan) with CuKα radiation.

Precise lattice parameter measurement was carried out for a cubic perovskite $BaCe_{0.9}Gd_{0.1}O_{2.95}$ phase using the following Nelson-Riley function:

$$\text{N.R.F.} = \frac{1}{2}\left(\frac{\cos^2\theta}{\sin\theta} + \frac{\cos^2\theta}{\theta}\right) \tag{4}$$

where θ is Bragg angle. The precise lattice parameter was determined by extrapolating the lattice parameter obtained at each diffraction peak to 90° (θ) in which the NRF value becomes zero. The measured 2θ values of diffraction peaks were calibrated with high purity Si powder (99.999%) as an external standard and the accuracy of the measurement was within ±0.001Å.

The concentrations of the nitrate solutions and the composition of the calcined powder were determined with an inductively coupled plasma spectrometer. The concentrations of Ba, Ce, and Gd nitrate solutions were found to be 0.04, 0.04 and 0.05M, respectively and the composition of the calcined powder coincided with the composition of $BaCe_{0.9}Gd_{0.1}O_{2.95}$.

Apparent densities of the calcined powders were measured with a helium gas pycnometer (AccuPyc 1330, Micromeritics, USA). Bulk densities of the sintered samples were determined with mercury porosimetry (PoreSizer 9320, Micromeritics, USA) and relative densities were calculated from the bulk density divided by the theoretical density (6.36 g/cm^3) which had been determined from the lattice parameter.

The powders and the sintered samples were examined with scanning electron microscopy (JSM-5410, JEOL, Japan). The sintered samples were polished and thermally etched at 100°C below each sintering temperature for 20 min in air.

III. Results and Discussion

1. Powder characterization

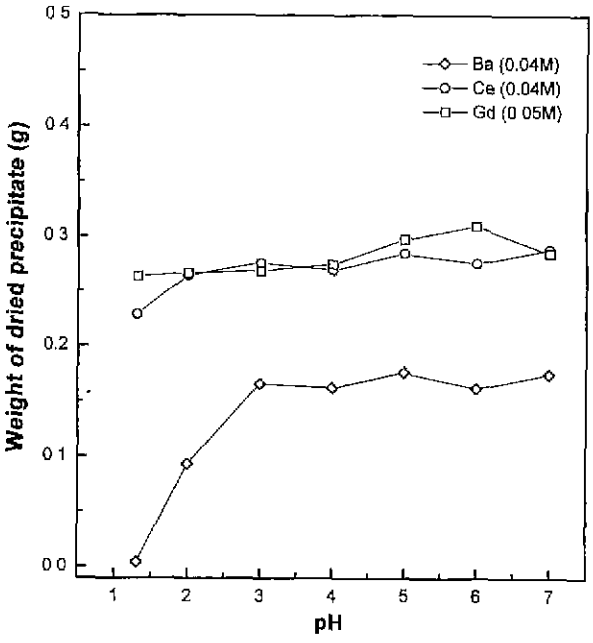

Fig. 1. Amount of dried precipitates obtained at various pH values of the oxalic acid solution.

For the preparation of the multicomponent Gd-doped barium cerate powder, precipitation reaction should be carried out under a condition that all metal ions do not precipitate into hydroxides but into oxalates. Fig. 1 shows the amounts of Ba, Ce and Gd precipitates obtained at various pH values of the oxalic acid solution. Ce and Gd ions precipitated at all pH values as compared to Ba ion. Ce and Gd ions are known to precipitate into hydroxides at pH>~6 and tend to form very stable complexes, ammonium oxalate hydrates ($NH_4Ce(C_2O_4)_2 \cdot H_2O$, $NH_4Gd(C_2O_4)_2 \cdot H_2O$), with an oxygen-donor ligand such as an oxalate ion ($C_2O_4^{2-}$) at pH≤~6.[17] Complete precipitation of Ba ions did not occur at pH<3, as shown by a sudden decrease in an amount of the precipitate with decreasing pH value. However, most Ba ions precipitated at pH≥3 as indicated by a constant amount of the precipitate. It has been reported that Ba oxalate hydrate ($BaC_2O_4 \cdot 0.5H_2O$) is formed at pH>2.[18] Therefore, it is anticipated that the precipitation at pH 4 results in chemically homogeneous precipitates.

The precipitates obtained at pH 1.3 (i.e., without adjusting pH) and 4 showed quite different thermal behaviors. TG/DTA curves of the precipitate obtained at pH 1.3 in Fig. 2(a) were found to be very similar to those of Ce oxalate hydrate, since the precipitate is Ba deficient and contains mostly Ce oxalate hydrate. Decomposition of the precipitate took place in two stages of a weight loss, 23.6% up to 202°C and 28.6% up to 500°C. An endothermic peak at 134°C is due to dehydration and decomposition of Ce ammonium oxalate hydrate and a strong exothermic peak at 316°C to decomposition of Ce oxalate.

Whereas, TG/DTA curves of the precipitate obtained at

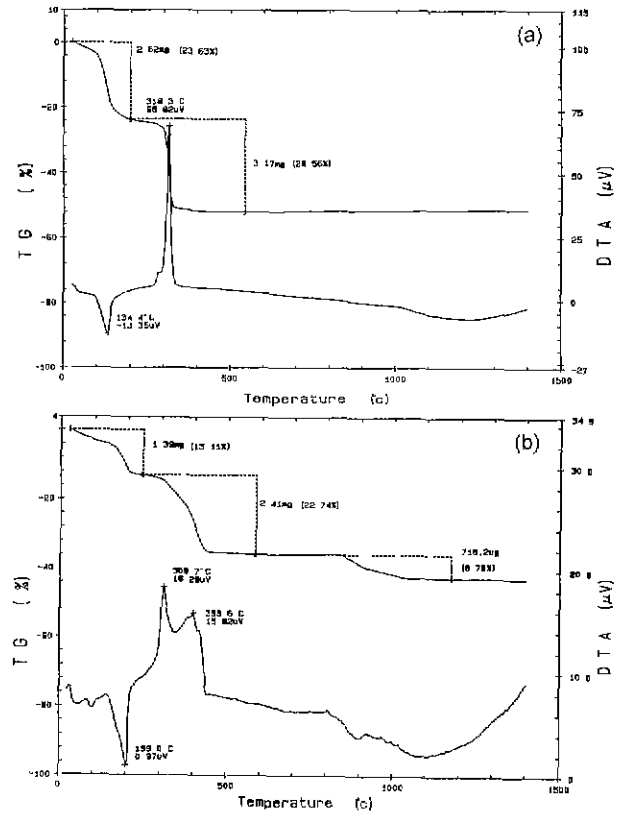

Fig. 2. TG/DTA curves of the precipitates obtained at (a) pH 1.3 (without adjusting pH) and (b) pH 4.

pH 4 in Fig. 2(b) exhibit three stages of a weight loss, which are related to decomposition reactions of the precipitate. A strong endothermic peak at 199°C is attributed to dehydration and decomposition of the hydrates of Ce ammonium oxalate and Ba oxalate, which is accompanied by 13.1% weight loss up to 232°C. Two strong exothermic peaks at 310° and 399°C correspond to decomposition of Ce and Ba oxalates, respectively. The decomposition reaction is strongly exothermic in air because of the oxidation of CO to CO_2. The decomposition of the oxalate is completed at temperature below ~450 °C, resulting in a 22.7% weight loss. A weight loss of 6.8% at temperature between 814°C and 1040°C arises from decomposition of $BaCO_3$. Weight changes similar to Fig. 2(b) have been reported by Flint and Slade,[11] who prepared Gd-doped barium cerate powder using an excess ammonium oxalate.

Ba deficiency in the precipitate obtained at pH 1.3 can be seen in XRD patterns of Fig. 3. In the powder heated at 400°C, $BaCO_3$ was not observed, but only CeO_2 appeared and persisted up to 1000°C. CeO_2 may exist with a small amount of Gd_2O_3 or as a solid solution since strong diffraction peaks owing to monoclinic Gd_2O_3 overlap CeO_2 peaks and Gd_2O_3 can form a solid solution with CeO_2 at 1000°C.

On the other hand, XRD patterns of the powder obtained at pH 4 in Fig. 4 show $BaCO_3$ and CeO_2 at 400

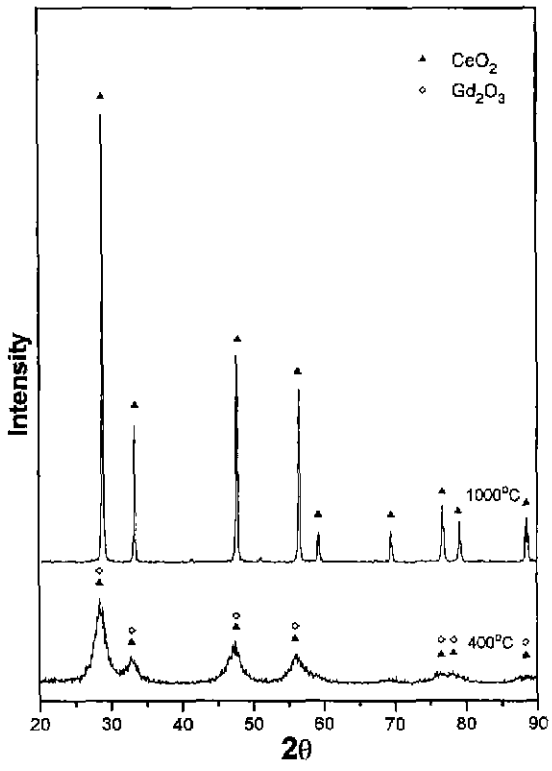

Fig. 3. XRD patterns of the powder precipitated at pH 1.3 and calcined at different temperatures for 4 h.

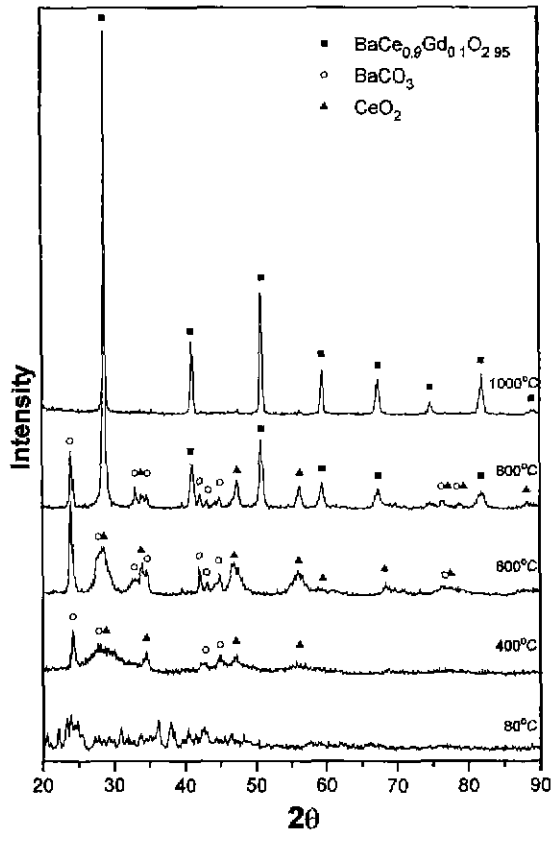

Fig. 4. XRD patterns of the powder precipitated at pH 4 and calcined at different temperatures for 4 h

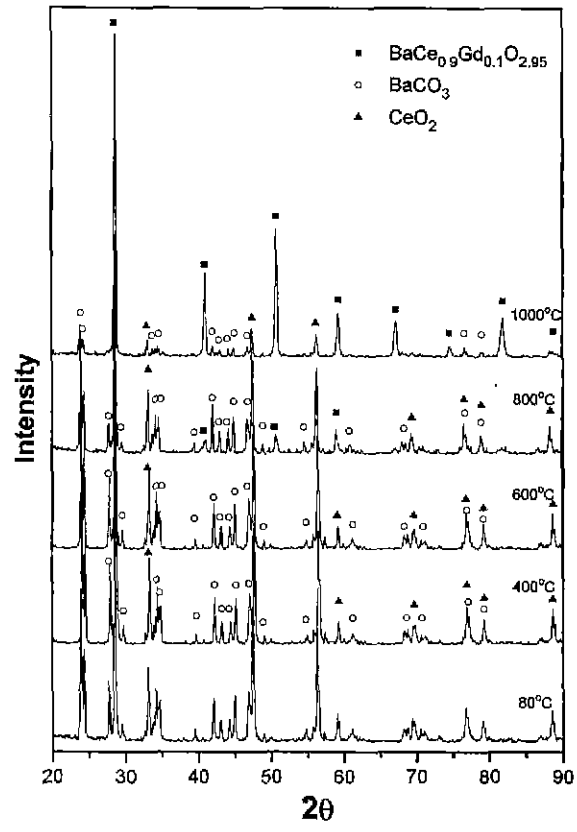

Fig. 5. XRD patterns of the powder prepared by solid state reaction and calcined at different temperatures for 4 h.

°C. Reaction between the constituent oxides was initiated at 800°C with concurrent decomposition of $BaCO_3$ and form a perovskite $BaCe_{0.9}Gd_{0.1}O_{2.95}$ phase. At 1000°C, a well-crystallized single perovskite phase developed, and $BaCO_3$ and CeO_2 completely disappeared.

The advantage of oxalate coprecipitation method over solid state reaction is illustrated by XRD patterns of the powder prepared by solid state reaction in Fig. 5. CeO_2, $BaCO_3$, and a perovskite $BaCe_{0.9}Gd_{0.1}O_{2.95}$ phase were present at 800°C as in the powder prepared by oxalate coprecipitation. However, $BaCO_3$ still remained up to 1000°C. It has been claimed that, for solid state reaction, calcination at temperatures above 1250°C is necessary in order to produce a single phase of $BaCe_{0.9}Gd_{0.1}O_{2.95}$ powder.[11] This temperature is at least ~250°C higher than required for oxalate coprecipitation method.

Fig. 6 is XRD pattern of the powder prepared by oxalate coprecipitation followed by calcination at 1000°C for 10 h. The diffraction peaks were indexed based on a cubic perovskite structure and the result is presented in Table 1. Weak diffraction peaks, not indexed in Fig. 6, are attributed to an orthorhombic structure. According to a recent neutron powder diffraction study, the structure of $BaCeO_3$ undergoes transformations from orthorhombic to rhombohedral at 400°C and to cubic structure at 900°C.[19] From an early XRD study, the structure of

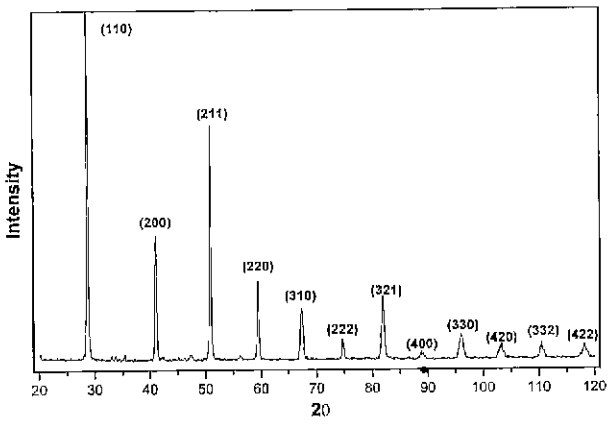

Fig. 6. XRD pattern of the powder prepared by oxalate coprecipitation and calcined at 1000°C for 10 h.

$BaCe_{0.9}Gd_{0.1}O_{2.95}$ has been reported to be cubic and isostructural with $BaCeO_3$.[20] However, a recent neutron powder diffraction study showed that the structure of $BaCe_{0.9}Gd_{0.1}O_{2.95}$ is orthorhombic with space group P_{bnm} and lattice parameters of a=6.23573(3)Å, b=6.21611(4)Å, and c=8.77697(5)Å.[15] The lattice parameter of the $BaCe_{0.9}Gd_{0.1}O_{2.95}$ phase in the powder prepared in this study was estimated according to a cubic unit cell and found to be 4.401±0.001Å. The lattice parameter and d-spacings in Table 1 are in good agreement with those reported by previous workers.[11,20] The volume of the cubic unit cell (85.2Å^3) is close to a 1/4 of the orthorhombic unit cell volume (340.2Å^3) and slightly larger than that (335.3Å^3) for $BaCeO_3$. Doping of $BaCeO_3$ for $BaCe_{0.9}Gd_{0.1}O_{2.95}$ has been found to cause a volume expansion of 2%.[20]

Table 1. X-Ray Diffraction Data* for $BaCe_{0.9}Gd_{0.1}O_{2.95}$ Powder**

h k l	d_{obs} (Å)	d_{cal} (Å)	I/I_o (Cukα_1)
1 1 0	3.105	3.112	100
2 0 0	2.199	2.201	17
2 1 1	1.794	1.797	31
2 2 0	1.554	1.556	10
3 1 0	1.391	1.392	6
2 2 2	1.270	1.270	2
3 2 1	1.176	1.176	5
4 0 0	1.101	1.100	7
3 3 0	1.037	1.037	0.5
4 2 0	0.983	0.984	3
3 3 2	0.938	0.938	2
4 2 2	0.899	0.898	1

*Indexing based on a cubic unit cell of a=4.401±0.001Å.
**Calcined at 1000°C for 10 h.

Fig. 7(a) is SEM micrograph of the precipitates, showing plate-shaped particles of submicron size. After calcination at 1000°C for 4 h, as shown in Fig. 7(b), the powder consisted of agglomerated particles and appeared to be porous due to the evolution of gases during decomposition. The powder could be milled with ease even after

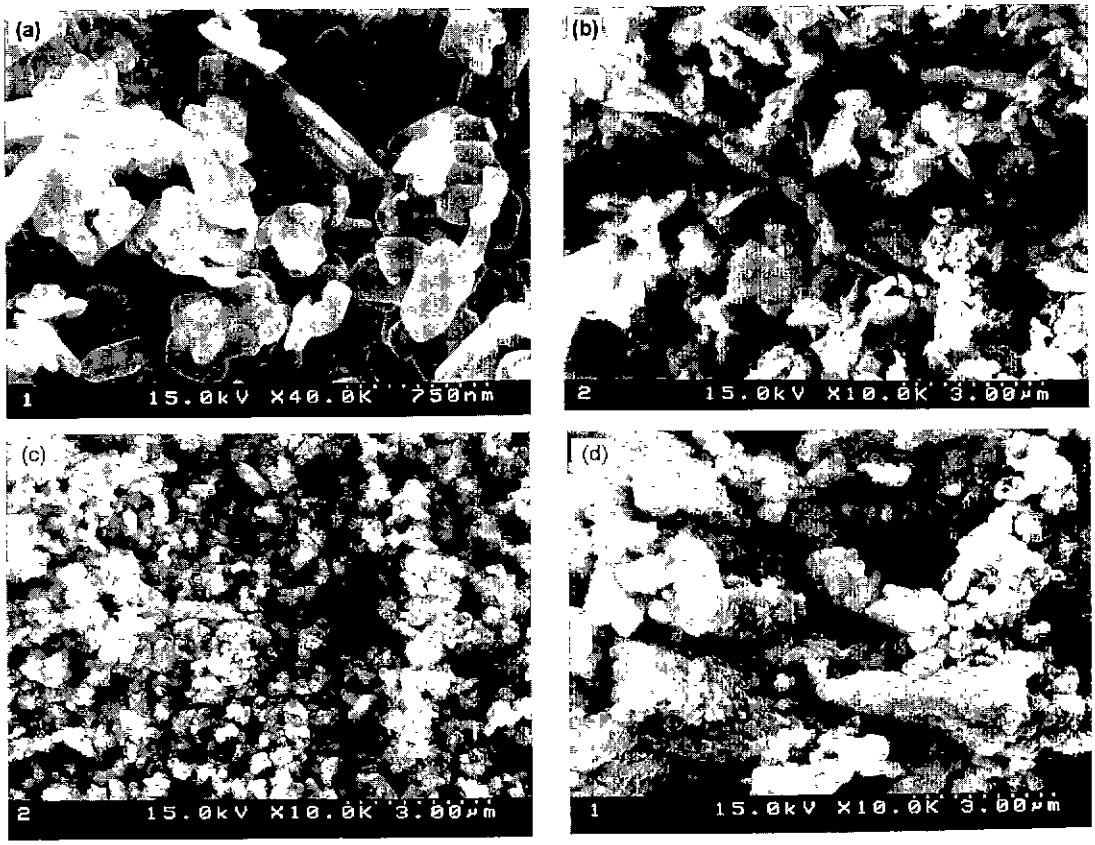

Fig. 7. SEM micrographs of (a) the precipitate dried at 80°C, (b) the powder calcined at 1000°C, (c) ball-milled powder and (d) ball-milled powder prepared by solid state reaction.

longer calcination time (10 h) at the same temperature. Fig. 7(c) exhibits the ball-milled powder containing some agglomerated particles. The powder had an average particle size of 0.2 μm and a size range of 0.08 μm to 1.12 μm. Apparent density of the powder was found to be 6.10 g/cm^3, 96% of the theoretical density. On the other hand, milling of the powder prepared by solid state reaction, shown in SEM micrograph of Fig. 7(d), seems to be very difficult owing to severe agglomeration between primary particles occurring during the high temperature calcination. The powder calcined at 1250°C for 10 h and ball-milled had an average particle size of 17.3 μm and a broad particle size distribution ranging from 0.3 μm to 171 μm.

2. Sintering and microstructure

Fig. 8 is the relative densities of samples sintered at various temperatures, suggesting that the powder prepared by oxalate coprecipitation has better sinterability than the powder prepared by solid state reaction. The relative densities of the green compacts prepared by oxalate coprecipitation and solid state reaction were found to be 61 and 63%, respectively. The sample prepared by oxalate coprecipitation shows that a considerable densification has already occurred at 1100°C, as indicated by nearly 79% relative density. As densification continued at higher temperatures, the density reached 93% at 1300°C and 97% at 1450°C. Flint and Slade,[11] who used oxalate coprecipitation method similar to this study, did not give definite density values and reported the density to be ≥80% after sintering at 1450°C for 10 h. In contrast, the samples prepared by solid state reaction did not show any significant densification up to 1200°C and had much lower relative density (78%) at

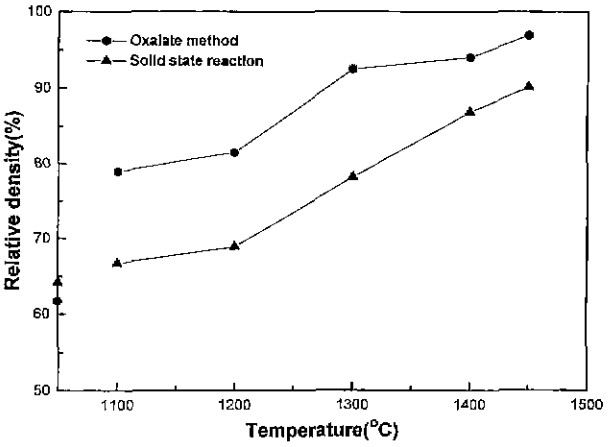

Fig. 8. Relative densities of sintered compacts of the powders prepared by oxalate coprecipitation and solid state reaction.

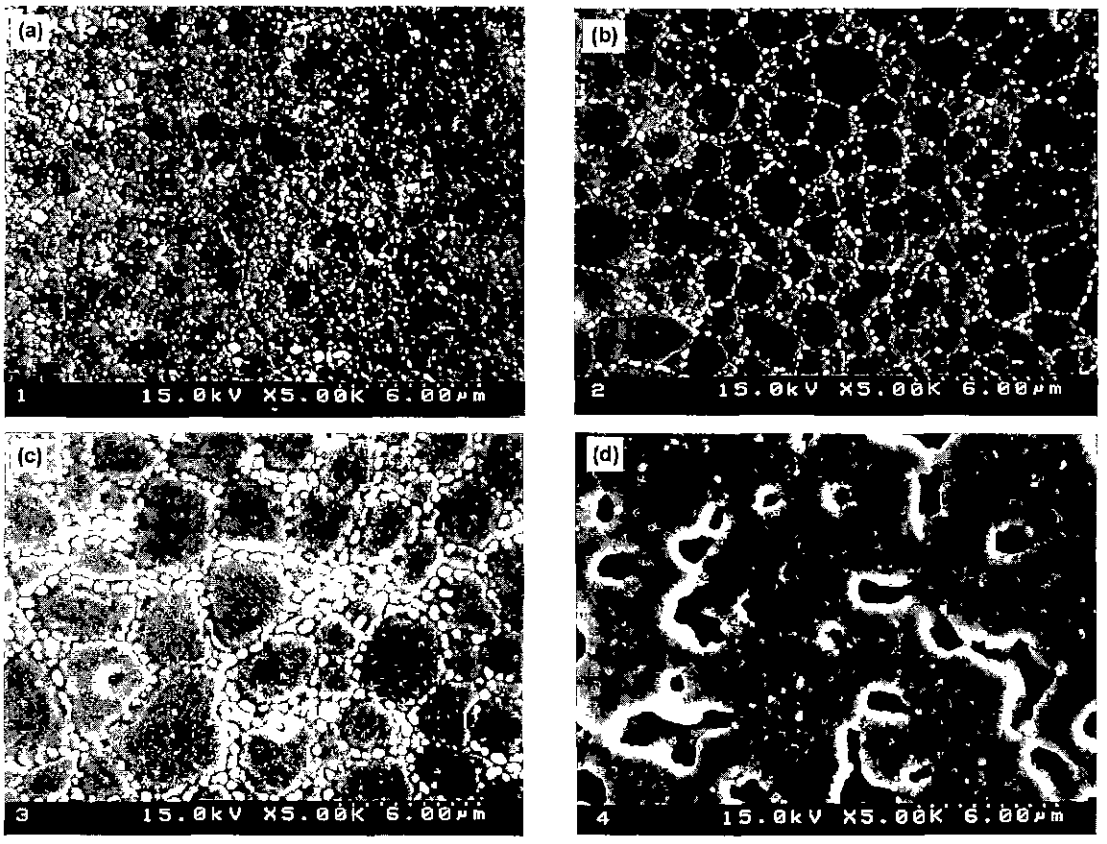

Fig. 9. SEM micrographs of the samples prepared by oxalate coprecipitation and sintered for 6 h at (a) 1300°C, (b) 1400°C, (c) 1450°C and (d) by solid state reaction and sintered at 1450°C for 6 h.

1300°C as compared to the sample prepared by oxalate coprecipitation. After sintering at 1450°C, the sample exhibited only 90% of the theoretical density.

Sintered densities of samples prepared by solid state reaction have been reported by many workers.[8,9,15,20] Stevenson et al.[8] found ~90% density after sintering at 1600°C. Kreuer et al.[9] and Shima and Haile[15] obtained 98~99% density at 1650°C. Whereas, Bonanos et al.[20] reported density in excess of 90% at 1475°C. Sintering at such high temperatures may not be appropriate for obtaining a dense and homogeneous microstructure. The high densities can be attributed to liquid phase sintering since an incongruent melting in the system BaO-CeO_2 is known to occur at 1480°C.[21] It should be noted that the density values determined by Hg porosimetry in the present study is more reliable than those reported by the other workers.[8,9,11,15] As pointed out previously, densities determined by sample weight and dimensions and by the Archimedes method can provide erroneous results. The Archimedes method has been tried, but it was observed that immersing the sample in water and boiling for elimination of air trapped in pores result in disintegration of the sample.

The surfaces of the sintered samples prepared by oxalate coprecipitation are shown in Fig. 9. The sample contained submicron sized grains at 1300°C (Fig. 9(a)). At 1400°C, fine particles of a second phase appeared around the matrix grains of 2~3 μm in size, as shown in Fig. 9(b). The second phase, which was not distinguishable from the matrix grains at 1300°C, grew to ~0.5 μm size around the matrix grains of 3~5 μm in size as the sintering temperature was raised to 1450°C (Fig. 9(c)). Fig. 9(d) is the surface of the sample prepared by solid state reaction and sintered 1450°C, exhibiting large pores and grains with nonuniform sizes. The second phase was not clearly visible in Fig. 9(d). Figs. 10 (a) and (b) show the different areas of the same samples as in Figs. 9 (c) and (d), respectively. In Fig. 10(a), the second phase particles were present either inside grains or at grain boundaries. In Fig. 10(b), the second phase particles were very fine and appeared at the grain boundaries in dense area, in contrast to the area that contained large pores as shown in Fig. 9(d).

The second phase particles were found to be present only on the surface of the samples. Figs. 11 (a) and (b) are the fractured surfaces of the sintered samples prepared by oxalate coprecipitation and by solid state reaction, respectively. In both samples, intragranular fracture occurred predominantly and the second phase particles were not observed inside or around the matrix grains. Results of energy dispersive X-ray microanalysis for both samples revealed that the second phase was deficient in BaO.

The second phase was identified with XRD of the surface of the sample prepared by oxalate coprecipitation and sintered at 1450°C. Fig. 12 (a) and (b) are the XRD patterns for the as-sintered surface of the sample and the polished and thermally etched surface of the sample, respectively. Both samples were sintered with being embedded in $BaCeO_3$ powder. In the as-sintered surface, only a perovskite $BaCe_{0.9}Gd_{0.1}O_{2.95}$ phase was detected (Fig. 12(a)), while in the polished surface of the sample CeO_2 appeared along with a perovskite $BaCe_{0.9}Gd_{0.1}O_{2.95}$ phase (Fig. 12(b)). The XRD pattern of the as-sintered surface of the sample without being embedded in $BaCeO_3$ powder, shown in Fig. 12(c), exhibits CeO_2 and a small amount of $BaCO_3$ beside a perovskite phase. XRD pattern of the

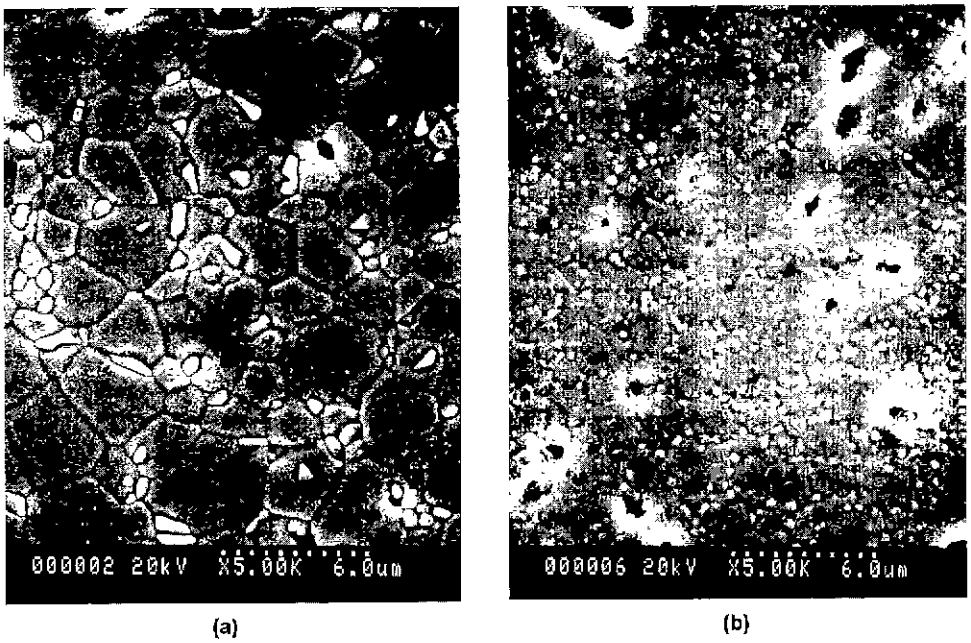

Fig. 10. SEM micrographs of the same samples as in Fig. 9 (c) and (d): (a) for oxalate coprecipitation and (b) for solid state reaction.

Fig. 11. SEM micrographs of fractured surfaces of the same samples as in Fig. 9 (c) and (d): (a) for oxalate coprecipitation and (b) for solid state reaction.

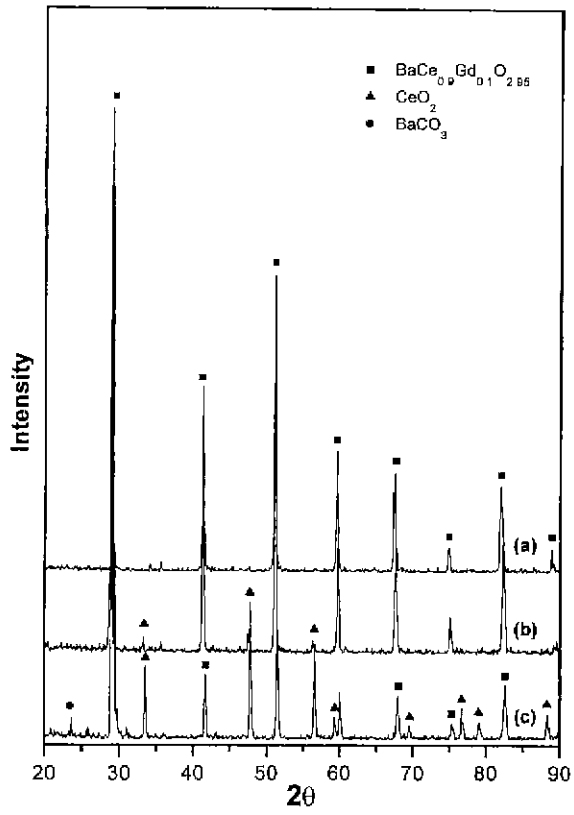

Fig. 12. XRD patterns for the surfaces of the samples sintered at 1450°C: (a) with being embedded in $BaCeO_3$ powder, (b) thermally etched surface of the sample (a) and (c) without being embedded in $BaCeO_3$ powder.

powdered samples showed only a single perovskite phase. These results suggest that the second phase is CeO_2 and attributed to the evaporation of BaO from the polished surface that has been exposed in air during thermal etching. The evaporation of BaO from the matrix phase near the grain boundaries can cause the decomposition of the matrix phase and leave excess CeO_2 at grain boundaries.

The evaporation of BaO during high temperature sintering ($\geq$1600°C) or after prolonged heat treatments has been reported. Shima and Haile[16] have found a weight loss of ~2 wt%, corresponding to ~5 mol% of BaO. Sintering over the incongruent melting temperature can cause a significant evaporation of BaO. Kreuer et al.[9] have observed a drop of the electrical conductivity of the doped barium cerates held at elevated temperatures for long periods of time and attributed this to a loss of BaO. In this study, the evaporation of BaO could be suppressed by sintering in an atmosphere controlled with $BaCeO_3$ powder. The second phase present in the surface has not been previously reported in any doped barium cerates. In Nd-doped barium cerates ($BaCe_{1-x}Nd_xO_{3-\alpha}$), a second phase containing excess Ce and Nd has been found to precipitate inside grains and at grain boundaries when a Nd content exceeds the solubility limit ($x \geq 0.2$).[13]

IV. Conclusion

Gd-doped barium cerate ($BaCe_{0.9}Gd_{0.1}O_{2.95}$) powder was synthesized by oxalate coprecipitation method and its characteristics and sinterability were investigated.

Oxalate precipitate having a stoichiometric ratio of the cations was prepared by adding a mixture of Ba, Ce, and Gd nitrate solutions to an oxalic acid solution at pH 4. The reaction between the constituent oxides to form a perovskite phase was initiated at 800°C. The pure and well-crystallized perovskite $BaCe_{0.9}Gd_{0.1}O_{2.95}$ powder was obtained after calcination at 1000°C, which is lower than required for the solid state reaction method. Sintering green compacts of this powder for 6 h showed a considerable densification to start at 1100°C and resulted in 93% and 97% relative densities at 1300°C and 1450°C, respectively. Whereas, the powder compacts prepared by solid state reaction had considerably lower relative densities, 78% at 1300°C and 90% at 1450°C.

Fine particles of CeO_2 second phase present at the grain boundaries were observed in the surfaces of the sintered compacts. This was attributed to the evaporation of BaO from the polished surface that had been exposed

in air during thermal etching.

Acknowledgment

This work was supported by the Ministry of Education Research Fund for Advanced Materials in 1996.

References

1. H. Iwahara, T. Eskar, H. Uchida and N. Maeda, "Proton Conduction in Sintered Oxides and Its Application to Steam Electrolysis for Hydrogen Production," *Solid State Ionics*, **3/4**, 359-363 (1981).
2. H. Iwahara, "Technological Challenges in the Application of Proton Conducting Ceramics," *Solid State Ionics*, **77**, 289-298 (1995).
3. N. Bonanos, K. S. Knight and B. Ellis, "Perovskite Solid Electrolytes· Structure, Transport Properties and Fuel Cell Applications," *Solid State Ionics*, **79**, 161-170 (1995).
4. K. D. Kreuer, "On the Development of Proton Conducting Materials for Technological Applications," *Solid State Ionics*, **97**, 1-15 (1997).
5. T. Schober, F. Krug and W. Schilling, "Criteria for the Application of High Temperature Proton Conductors in SOFCs," *Solid State Ionics*, **97**, 369-373 (1997).
6. N. Bonanos, "Transport Properties and Conduction Mechanism in High-Temperature Protonic Conductors," *Solid State Ionics*, **53-56**, 967-974 (1992).
7. J. F. Liu and A. S. Nowick, "The Incorporation and Migration of Protons in Nd-doped $BaCeO_3$," *Solid State Ionics*, **50**, 131-38 (1992).
8. D. A. Stevenson, N. Jiang, R. M. Buchanan and F. E. G. Henn, "Characterization of Gd, Yb and Nd Doped Barium Cerates as Proton Conductors," *Solid State Ionics*, **62**, 279-285 (1993).
9. K. D. Kreuer, E. Schönherr and J. Maier, "Proton and Oxygen Diffusion in $BaCeO_3$ Based Compounds: A Combined Thermal Gravimetric Analysis and Conductivity," *Solid State Ionics*, **70/71**, 278-284 (1994).
10. H. Iwahara, T. Mori and T. Hibino, "Electrochemical Studies on Ionic Conduction in Ca-Doped $BaCeO_3$," *Solid State Ionics*, **79**, 177-182 (1995).
11. S. D. Flint and R. C. T. Slade, "Comparison of Calcium-Doped Barium Cerate Solid Electrolytes Prepared by Different Routes," *Solid State Ionics*, **77**, 215-221 (1993).
12. F. Chen, O. T. Sørensen, G. Meng and D. Peng, "Preparation of Nd-Doped Barium Cerate Through Different Routes," *Solid State Ionics*, **100**, 63-72 (1997).
13. C.-H. Lu and L. C. De Jonghe, "Influence of Nd_2O_3 Doping on the Reaction Process and Sintering Behavior of $BaCeO_3$ Ceramics," *J. Am. Ceram. Soc.*, **77**(10), 2523-2528 (1994).
14. S. D. Flint, M. Hartmanová, J S. Jones and R. C. T. Slade, "Microstructure of Ca-Doped Barium Cerate Electrolytes $BaCe_{1-x}Ca_xO_{3-\alpha}$ (x=0, 0.02, 0.05, 0.10 and 0.15)," *Solid State Ionics*, **86-88**, 679-683 (1996).
15. D. Shima and S. M. Haile, "The Influence of Cation Non-Stoichiometry on the Properties of Undoped and Gadolinia-Doped Barium Cerate," *Solid State Ionics*, **97**, 443-455 (1997).
16. E. Zimmer, K. Scharf, T. Mono, J. Friedrich and T. Schober, "Preparation of the High Temperature Proton Conductor $Ba_3Ca_{1.18}Nb_{1.82}O_{8.73}$ via a Wet Chemical Route," *Solid State Ionics*, **97**, 505-509 (1997).
17. C. F. Baes, Jr. and R. E. Mesner, The Hydrolysis of Cation, pp. 129-139, John Wiley & Sons, Inc. New York, 1976.
18. T. T. Fang and H. B. Lin, "Factors Affecting the Preparation of Barium Titanyl Oxalate Tetrahydrate," *J. Am. Ceram. Soc.*, **72**(10), 1899-1906 (1989).
19. K. S. Knight, "Structural Phase Transitions in $BaCeO_3$," *Solid State Ionics*, **74**, 109-117 (1994).
20. N. Bonanos, B. Ellis, K. S. Knight and M. N. Mahmood, "Ionic Conductivity of Gadolium-Doped Barium Cerate Perovskites," *Solid State Ionics*, **35**, 179-188 (1989).
21. G. P. Guha and D. Kolar, "Phase Equilibria in the System $BaO-CeO_2$," *J. Mater. Sci.*, **6**(9), 1174-1177 (1971).